



O. Steiner & J. Bruls, *Kiepenheuer-Institut fuer Sonnenphysik, Freiburg*
P.H. Hauschildt, *University of Georgia, Athens, USA*

1. The G-band and G-band bright-points

The *G-band* is a molecular bandhead in the solar spectrum at 430 ± 1 nm characterized by electronic transitions from and to rotational and vibrational sublevels of the molecule CH. At low spectral resolution the bandhead looks like a single spectral line, labeled "G" by Fraunhofer (1814).

"G-band bright points" are small (≤ 200 km) magnetic structures, *magnetic elements*, that appear conspicuously bright when observed with a G-band-pass filter. They are concentrations of magnetic flux into tube-like structures in the photosphere.

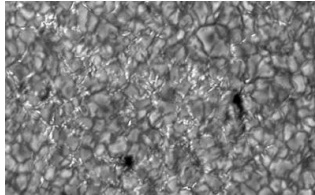


Fig. 1. G-band filtergram obtained with the German Vacuum-Tower Telescope on Tenerife and the Adaptive-Optics System of the Sacramento-Peak Observatory. G-band bright points are visible as "strings of beads" in many locations of intergranular lanes. (Observations by von der Luehe *et al.*)

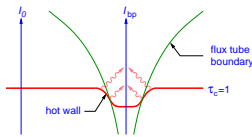


Fig. 2. Sketch of a *magnetic flux tube* representing a magnetic element at the solar surface. The $\tau_c = 1$ -surface is depressed at the location of the tube, which exposes hot subsurface material at the circumference of the depression, where excessive radiative cooling takes place. Also indicated are representative lines-of-sight for computation of the synthetic spectra.

What causes the high contrast of magnetic elements in the G-band? There exist several propositions aiming at an explanation of this effect (see Rutten 1999). We test the following hypothesis:

The elevated temperature of bright points (with respect to their surroundings), enhances CH-dissociation causing a reduction of CH-line depths and consequently a higher intensity in the G-band.

This hypothesis does not involve any NLTE-effects.

2. Model and model atmospheres

In this study, the geometrical structure of the magnetic flux tubes is discarded but instead, their atmosphere considered to be *plane-parallel*. Correspondingly, synthetic results will be compared with contrast measurements that are corrected for the limited spatial resolution by means of instrumental and atmospheric modulation transfer functions, *i.e.*, with intrinsic contrast values.

We use the empirically derived *model atmospheres* for magnetic elements of network (net) and plage (pla) regions of Solanki & Brigrjevic (1992) and compare the resulting spectra with that of the surrounding quiet Sun reference atmosphere (FWFAK.C) of Fontenla *et al.* (1999).

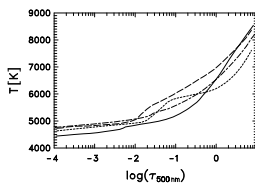


Fig. 3. Temperature as a function of continuum optical depth $\tau_{500\text{nm}}$ of the modified quiet Sun model FWFAK.C (—) and the bright plage model FWFAK.P (---) of Fontenla *et al.* 1999, together with the magnetic flux tube atmospheres net (network elements, - - -) and pla (plage elements,) of Solanki & Brigrjevic (1992).

3. Synthetic G-band spectrum

We use the radiation transfer code PHOENIX (Hauschildt & *et al.* 1996, 97, 99) in order to compute synthetic G-band spectra and the continuum radiation from each model atmosphere. Line profiles are depth-dependent Voigt profiles, or Doppler profiles

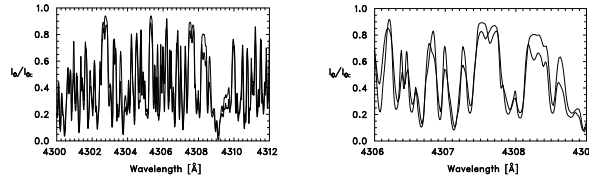


Fig. 4. Left: Synthetic G-band spectrum from the quiet-Sun model atmosphere (bold curve) together with the corresponding section of the "Jungfraujoch" spectral atlas (thin curve). Right: Detailed comparison from 430.6 to 430.9 nm.

4. Synthetic G-band contrast

Figure 5 shows the synthetic G-band spectrum of the magnetic-element model (red), together with that of the quiet Sun model (blue) and with the continuum intensity attenuated by the transmission profile of the G-band pass filter (dashed). The magnetic element shows a higher intensity throughout because it is hotter than the quiet Sun model, but the difference is more pronounced within ranges of CH-band lines than in the continuum and many other spectral lines.

Table 1 gives contrasts for three model atmospheres against the quiet Sun reference, where

for very weak lines. We use a height-independent microturbulence of 1 km s^{-1} . Figures 4 shows a comparison between the synthetic spectrum (bold curve) and the corresponding section of the "Jungfraujoch"-atlas (Delbouille *et al.* 1989).

$$C_c = \frac{(I_{bp,c} - I_{0,c})}{I_{0,c}}, \quad \text{and} \quad C_G = \frac{\int T_G(I_{bp} - I_0) d\lambda}{\int T_G I_0 d\lambda}$$

Index *c* refers to the theoretical continuum at 430 nm, bp to the flux-tube atmosphere, and 0 to the quiet Sun model. T_G is the G-band filter transmission. C_G is the "G-band" contrast when discarding the molecule CH in the radiation transfer.

	net	pla	FWFAK.P
C_G	1.34	0.28	0.39
C_c	0.33	-0.22	-0.03
C_G^c	0.66	-0.05	0.12

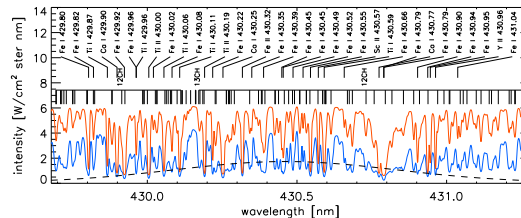


Fig. 5. Synthetic G-band spectrum of the quiet Sun model FWFAK.C (blue curve) together with that of the magnetic-element atmosphere net (Solanki & Brigrjevic 1992) (red curve) and the continuum intensity attenuated by the transmission profile of the G-band pass filter (dashed curve).

5. What causes the high G-band contrast?

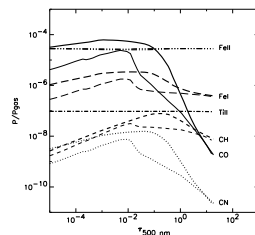


Fig. 6. Partial gas pressure for the molecules CO, CH, and CN as a function of optical depth $\tau_{500\text{nm}}$. Thick curves refer to the quiet Sun model, thin curves to the magnetic-element atmosphere. The partial pressures of Fe I, Fe II, and Ti II, are practically identical and constant for both atmospheres.

6. Conclusion

The high contrast in the G-band is largely a consequence of the CH depletion through molecular dissociation in the deep photospheric layers of the flux-tube atmospheres that is hot compared to the quiet Sun surroundings.

Other molecular bandheads and many (weak) Fe I and other neutral metal lines across the spectrum are expected to behave similar to the CH-lines of the G-band.

The conjecture of Rutten (1999) that photodissociation by UV-radiation from the hot flux-tube walls are an important mechanism of G-band contrast enhancement cannot be falsified. However, we show that dissociation processes in LTE suffice to produce the observed contrast enhancement.

From Fig. 6 we see:

- CH increases with height less steep than CO because CO curtails the formation of CH with height. \rightarrow Deep formation of the G-band. The CH line-cores form around $\tau_{500\text{nm}} = 0.1$.
- The CH partial pressure of the flux-tube atmosphere is markedly reduced w.r.t. the reference atmosphere in the deep layers. This reduction is due to the elevated temperature of up to 800 K within the flux tube, causing CH to dissociate. This weakens the CH lines in the G-band of magnetic elements, allowing more of the continuum to "shine through the thinned forest" of CH-lines. \rightarrow The high contrast of G-band bright-points is due to the depletion of CH, induced by the enhanced temperature of magnetic elements.
- Fe I behaves similar to CH. \rightarrow The multitude of Fe I lines within the G-band also contributes to the contrast enhancement. This is the reason for $C_G^c > C_c$.

7. References

Delbouille, L., Roland, G., & Neven, L. 1989, Photometrie Atlas of the Solar Spectrum (Univ. de Liege)
Fontenla, J., White, O. R., Fox, P. A., Avrett, E. H., & Kurucz, R. L. 1999, ApJ, 518, 480
Hauschildt, P. H., Baron, E., Starrfeld, S., & Allard, F. 1996, ApJ, 462, 386
Hauschildt, P. H., Allard, F., & Baron, E. 1999, ApJ, 512, 377
Hauschildt, P. H., Baron, E., & Allard, F. 1997, ApJ, 483, 390
Rutten, R., Kiselman, D., Rouppé van der Voort, L., & Plez, B. 2001, in ASP Conf. Ser., Vol. 236, Advanced Solar Polarimetry, M. Sigwarth (ed.), 445-452
Rutten, R. J. 1999, in ASP Conf. Ser., Vol. 184, Magnetic Fields and Oscillations, B. Schmieder, A. Hoffmann, & J. Staudé (eds), 181-200
Sánchez Almeida, J., Asensio Ramos, A., Trujillo Bueno, J., & Cernicharo, J. 2001, ApJ, 555, 978
Solanki, S. K. & Brigrjevic, V. 1992, A&A, 262, L29
Steiner, O., Hauschildt, P. & Bruls, J. 2001, A&A, 372, L13